PROTOTYPE FILTER DESIGN FOR FILTER BANK BASED MULTICARRIER TRANSMISSION

Ari Viholainen[†], *Tero Ihalainen*[†], *Tobias Hidalgo Stitz*[†], *Markku Renfors*[†], *and Maurice Bellanger*[⋆]

[†]Department of Communications Engineering, Tampere University of Technology
P.O. Box 553, FI-33101 Tampere, Finland, Email: {ari.viholainen, tero.j.ihalainen, tobias.hidalgo, markku.renfors}@tut.fi

[⋆]CNAM, 292 rue Saint-Martin, 75141 Paris cedex 03, France, Email: bellang@cnam.fr

ABSTRACT

This paper concentrates on an efficient prototype filter design in the context of filter bank based multicarrier (FBMC) transmission. An advantage of the chosen method, frequency sampling technique, is that near perfect reconstruction prototype filters can be expressed using a closed-form representation with only a few adjustable parameters. The performance of various designs are analyzed using the offset-QAM based FBMC system. Numerical results are provided to characterize different optimization criteria in terms of frequency selectivity of resulting prototype filters and total interference level of the filter bank structure. Furthermore, it is shown what kind of performance trade-offs can be obtained by adjusting those free parameters. In this sense, the presented results offer useful information to a system designer.

1. INTRODUCTION

Multicarrier modulation is an efficient transmission technique, where the available channel bandwidth is subdivided into several parallel subchannels, each with its own associated carrier. In filter bank based multicarrier (FBMC) modulation techniques, a synthesis-analysis filter bank, i.e., transmultiplexer (TMUX) structure can be considered to be the core of a system. The synthesis filter bank (SFB) consists of all parallel transmit filters and the analysis filter bank (AFB) includes the matching receive filters. Typically, modulated filter banks are used as a computationally efficient solution whenever filter banks are needed [1].

There are many different kinds of multicarrier techniques, but orthogonal frequency division multiplexing (OFDM) has been, no doubt, the most prominent solution [2]. From the filter bank point of view, conventional OFDM is based on a rectangular prototype filter and IFFT/FFT blocks. The resulting subchannel filters are not very frequency selective because the first sidelobe is only 13 dB below the mainlobe. More recently, alternative techniques, such as filtered multitone (FMT) [3], cosine modulated multitone (CMT) [4], OFDM with offset QAM (OFDM/OQAM) based technique [5], modified DFT (MDFT) based technique [6], and exponentially modulated filter bank (EMFB) based technique [7], have been proposed in the context of different applications. The distinctive feature of these FBMC techniques is their ability to provide improved frequency selectivity through the use of longer and spectrally well-shaped prototype filters.

This research was supported in part by the European Commission under Project PHYDYAS (FP7-ICT-2007-1-211887). Tero Ihalainen's work was additionally supported by TISE graduate school.

The design of a TMUX mainly concentrates on the prototype filter design because all subchannel filters are generated from this prototype filter. In practical applications, the number of needed subchannels M can be hundreds or even thousands. Such a demand turns the design process very complicated because, typically, filter lengths somehow depend on the number of subchannels (e.g., $L_p = KM - 1$, where K is a positive integer). Therefore, design techniques that can reduce the number of parameters to be optimized are particularly interesting. In this paper, the potential of a frequency-domain technique, called as frequency sampling technique [8], is studied. Its main advantage is that a prototype filter can be expressed using scalable closed-form formula that only depends on a few adjustable parameters.

The rest of this paper is organized as follows: Section 2 describes a TMUX configuration that utilizes offset-QAM model for subcarrier modulation[1]. In Section 3, the basic idea of a frequency sampling technique is recalled. Section 4 concentrates on the optimization of prototype filters and the problem is considered from the design criteria point of view. Optimization results and important observations are presented in Section 5. Finally, concluding remarks are summarized in Section 6.

2. TMUX MODEL

The core of the FBMC/OQAM system is a critically sampled TMUX configuration shown in Fig. 1. The main processing blocks are OQAM pre-processing, SFB, AFB, and OQAM post-processing. The transmission channel is typically assumed to be ideal ($C(z) = 1$) when analyzing and designing TMUX systems because the channel equalization problem is handled separately.

In order to guarantee downsampling at correct phase (at the maximum points of the received pulses), an extra delay z^{-D}, with D depending on the length of the prototype filter

$$L_p = KM + 1 - D, \tag{1}$$

has to be included either to the SFB output or AFB input [5]. This paper concentrates on the specific prototype filter length of $L_p = KM - 1$. Based on Eq. (1), the required extra delay in the TMUX system is z^{-2}. A simple implementation method for this delay is to insert an additional zero coefficient to the beginning of the impulse response of the optimized prototype filter.

[1]Noting that the OFDM/OQAM model is essentially equivalent to the MDFT filter bank model, it can be stated that the OFDM/OQAM model is clearly the most common FBMC principle considered in the literature. Hereafter, this principle is referred to as FBMC/OQAM.

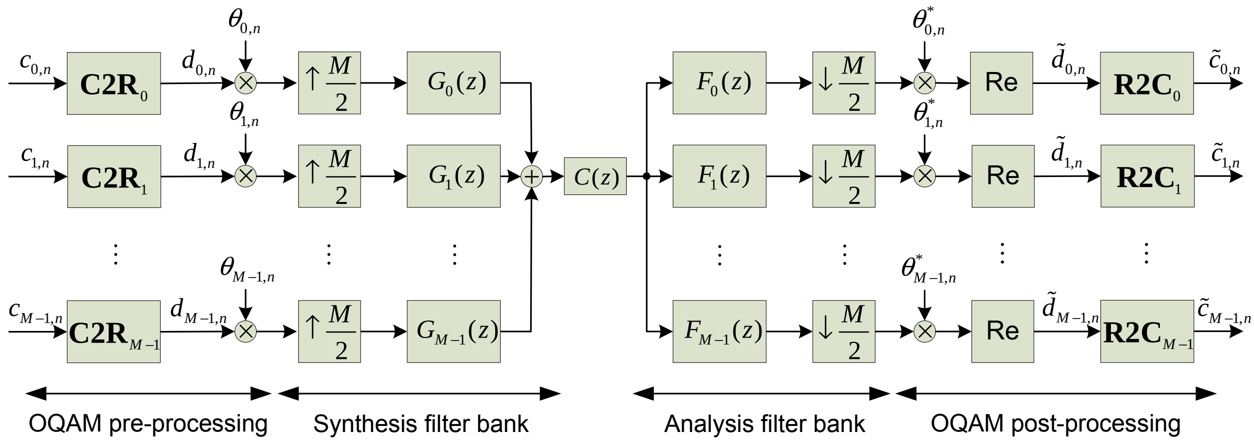

Figure 1: Direct form representation of TMUX model.

2.1 OQAM pre-processing

The first operation is a complex-to-real conversion ($\mathbf{C2R}_k$), where the real and imaginary parts of a complex-valued symbol $c_{k,n}$ are separated to form two new symbols

$$d_{k,2n} = \begin{cases} \mathrm{Re}[c_{k,n}], & k \text{ even} \\ \mathrm{Im}[c_{k,n}], & k \text{ odd} \end{cases} \tag{2}$$

and

$$d_{k,2n+1} = \begin{cases} \mathrm{Im}[c_{k,n}], & k \text{ even} \\ \mathrm{Re}[c_{k,n}], & k \text{ odd.} \end{cases} \tag{3}$$

This means that the complex-to-real conversion increases the sample rate by a factor of 2. The second operation in this OQAM pre-processing is the multiplication by a sequence

$$\theta_{k,n} = e^{j\frac{\pi}{2}(k+n)} = j^{(k+n)}. \tag{4}$$

It should be noted that the signs of the sequence can be chosen arbitrarily, but the pattern of real and imaginary samples has to follow the above definition [5].

2.2 Synthesis and analysis filter banks

In the SFB, the input signals are first upsampled by $M/2$ and then filtered with synthesis filters $G_k(z)$. The SFB output signal is formed when all subsignals are added together. In the AFB, the input signal is first filtered by analysis filters $F_k(z)$ and these signals are then downsampled by a factor of $M/2$ to form output signals. The presented TMUX system can be considered to be critically sampled because the sample rate (counted in terms of real-valued samples) of the SFB output (AFB input) is equal to the sum of the sample rates of the subchannel signals $d_{k,n}$ ($\tilde{d}_{k,n}$).

In the case of chosen class of complex modulated filter banks, all subchannel filters can be generated from a single real-valued linear-phase FIR lowpass prototype filter $p[m]$ by using exponential modulation as follows

$$f_k[m] = p[m]e^{j\left(\frac{2\pi k}{M}\left(m-\frac{L_p-1}{2}\right)\right)} \tag{5}$$

and

$$h_k[m] = f_k^*[L_p-1-m] = p[m]e^{j\left(\frac{2\pi k}{M}\left(m-\frac{L_p-1}{2}\right)\right)}, \tag{6}$$

where $k = 0,1,\ldots,M-1$ and $m = 0,1,\ldots,L_p-1$. Due to the modulation function, the resulting subchannel filters have also linear phase.

The magnitude response of the prototype filter is divided into three types of regions: the passband region is $[0,\omega_p]$, the stopband region is $[\omega_s,\pi]$, and the gap between these two is called as the transition band. The band edges can be given as follows $\omega_p = \frac{(1-\alpha)\pi}{M}$ and $\omega_s = \frac{(1+\alpha)\pi}{M}$, where α is the roll-off factor that defines how much adjacent subchannels are overlapping. A typical choice is $\alpha = 1.0$, which means that the transition bands of a subchannel end at the centers of the adjacent subchannels.

2.3 OQAM post-processing

There are again two slightly different structures depending on the subchannel index. The first operation is the multiplication by $\theta^*_{k,n}$ sequence that is followed by the operation of taking the real part. The second operation is real-to-complex conversion ($\mathbf{R2C}_k$), in which two successive real-valued symbols (with one multiplied by j) form a complex-valued symbol $\tilde{c}_{k,n}$, i.e.,

$$\tilde{c}_{k,n} = \begin{cases} \tilde{d}_{k,2n} + j\tilde{d}_{k,2n+1}, & k \text{ even} \\ \tilde{d}_{k,2n+1} + j\tilde{d}_{k,2n}, & k \text{ odd.} \end{cases} \tag{7}$$

In this sense, the real-to-complex conversion decreases the sample rate by a factor 2.

3. FREQUENCY SAMPLING DESIGN TECHNIQUE

The prototype filter can be designed to fulfill PR conditions or to provide NPR characteristics. However, it is worth emphasizing that the PR property is exactly obtained only in the case of ideal transmission channel. Therefore, it is sufficient that interferences that originate from the filter bank structure are small enough compared to the residual interferences due to transmission channel. In addition, NPR prototype filters can provide higher stopband attenuation than their equal-length PR counterparts.

A straightforward way to design NPR prototype filters is to directly optimize the impulse response coefficients. An evident drawback of this approach is that the number of filter coefficients increases dramatically when designing filter banks with high number of subchannels ($M > 128$). Another approach is to use e.g., frequency sampling technique [9] or windowing based techniques [10]. In these methods, prototype filter coefficients can be given using a closed-form representation that includes only a few adjustable design parameters.

This paper concentrates on the frequency sampling technique. The general idea is very simple: the impulse response coefficients of a filter are obtained when the desired frequency response, which is sampled on a KM uniformly spaced frequency points $\omega_k = \frac{2\pi k}{KM}$, is inverse Fourier transformed [8]. The resulting closed-form representation for a real-valued symmetric FIR prototype filter can be written as[2]

$$p[m] = \frac{1}{KM}\Big(A[0] + 2\sum_{k=1}^{U}(-1)^k A[k]\cos\Big(\frac{2\pi k}{KM}(m+1)\Big)\Big), \quad (8)$$

where $m = 0,1,\ldots,KM-2$, $U = \frac{KM-2}{2}$, and the coefficients $A[k]$ are the desired values of the frequency response.

In order to obtain a proper lowpass prototype filter, the magnitude response of the filter should achieve the value of 1 at $\omega = 0$ and at least approximately the value of $1/\sqrt{2}$ at $\omega = \pi/M$. Furthermore, the stopband attenuation should be as high as possible. As shown in [6], the following choices guarantee these requirements:

$$\begin{cases} A[0] = 1 \\ A[l]^2 + A[K-l]^2 = 1, \text{ for } l = 1,2,\ldots,\lfloor K/2 \rfloor \\ A[l] = 0, \text{ for } l = K, K+1, \ldots, U. \end{cases} \quad (9)$$

In this manner, the number of adjustable parameters is considerably reduced. For example, there is only one free parameter when $K = 3$ and $K = 4$:

- $K = 3$: $A[0] = 1, A[1] = x, A[2] = \sqrt{1-x^2}$
- $K = 4$: $A[0] = 1, A[1] = x, A[2] = 1/\sqrt{2}, A[3] = \sqrt{1-x^2}$.

The goal of the optimization is to find out the coefficient $A[1]$ in such a manner that the selected optimization criterion is minimized. In this case, it is even possible to use simple global search to track down the optimum solution.

4. OPTIMIZATION CRITERIA

In many cases, the constraints imposed by the problem automatically shape the passband region and only the stopband region is taken into account in the objective function. Three well-known frequency-domain design criteria are the least-squares (LS), minimax, and peak-constrained least-squares (PCLS) criteria. In addition, we introduce the total interference, which originates from the filter bank structure, as a new criterion.

4.1 Least-squares criterion (C1)

The goal of the LS criterion is to minimize the stopband energy of the prototype filter. The objective function can be written as follows

$$F(\mathbf{x}) = \int_{\omega_s}^{\pi} |P(e^{j\omega})|^2 d\omega. \quad (10)$$

This criterion is also known as the L_2 norm.

[2] Here, the exact mathematical derivation is omitted, however, an interested reader can refer to [8, 11] where the filter length $L_p = KM$ is considered.

4.2 Minimax criterion (C2)

The goal of the minimax criterion is to minimize the maximum stopband ripple instead of the stopband energy. In minimax design, the objective function is

$$F(\mathbf{x}) = \max_{\omega \in [\omega_s, \pi]} |P(e^{j\omega})|. \quad (11)$$

This criterion is also known as the Chebyshev design criterion or the L_∞ norm.

4.3 Peak-constrained least-squares criterion (C3)

The PCLS criterion offers a trade-off between the LS and minimax criteria. The objective function is the stopband energy (shown in Eq. (10)) subject to maximum stopband ripple that is less than or equal to some prescribed value δ, i.e., $|P(e^{j\omega})| \le \delta$ for $\omega \in [\omega_s, \pi]$. If δ is large enough, then this criterion reduces to the LS criterion. When decreasing δ, this criterion approaches the minimax criterion.

4.4 Total interference criterion (C4)

The goal of this criterion is to minimize the total interference that originates from the filter bank structure. In this case, the objective function can be written as follows

$$F(\mathbf{x}) = \mathrm{ISI} + \mathrm{ICI}, \quad (12)$$

where the terms ISI and ICI stand for intersymbol interference and intercarrier interference, respectively. They can be measured by forming the input-output relation of the corresponding FBMC system. In the case of FBMC/OQAM, it is advantageous to include multipliers $\theta_{k,n}$, $\theta^*_{k,n}$, and Re-operations to the TMUX configuration, i.e., the considered input and output signals are purely real-valued as is the case also in [5].

The transfer functions between real-valued input and output signals can be collected together using matrix notations as follows

$$\tilde{\mathbf{D}}(z^{M/2}) = \mathbf{T}_{TMUX}(z^{M/2}) \cdot \mathbf{D}(z^{M/2}) \quad (13)$$

where

$$\tilde{\mathbf{D}}(z) = \big[\tilde{D}_0(z) \;\; \tilde{D}_1(z) \;\; \cdots \;\; \tilde{D}_{M-1}(z)\big]^T, \quad (14)$$

and

$$\mathbf{D}(z) = \big[D_0(z) \;\; D_1(z) \;\; \cdots \;\; D_{M-1}(z)\big]^T. \quad (15)$$

The matrix $\mathbf{T}_{TMUX}(z^{M/2})$ is the transfer matrix and its element $\big[\mathbf{T}_{TMUX}(z^{M/2})\big]_{a,b}$ represents the relation between input signal $D_b(z^{M/2})$ and the output signal $\tilde{D}_a(z^{M/2})$. The elements in the main diagonal are the transfer functions of the subchannels of the TMUX system and other elements describe the crosstalk between different subchannels.

The powers of the interference components due to filter bank structure based ISI and ICI can be estimated for example by using the following formula

$$\mathrm{ISI} = \max_k \Big(\sum_n ([\mathbf{T}_{TMUX}(n)]_{k,k} - \delta(n-\Delta))^2\Big) \quad (16)$$

and

$$\mathrm{ICI} = \max_k \Big(\sum_{l=0, l\neq k}^{M-1} \sum_n ([T_{TMUX}(n)]_{k,l})^2\Big). \quad (17)$$

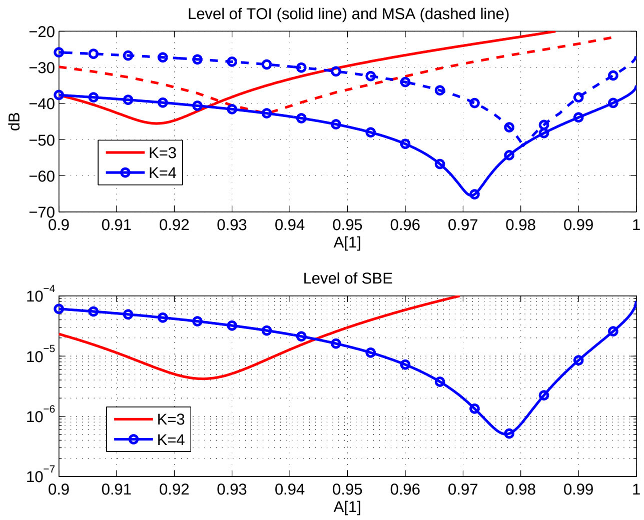

Figure 2: Level of TOI, MSA, and SBE as a function of parameter $A[1]$.

Here, $\delta(n)$ is the ideal impulse and Δ is the delay of TMUX system. In the case of FBMC/OQAM, crosstalk terms $\left[\mathbf{T}_{TMUX}(z^{M/2})\right]_{a,b} = 0$ if $a+b$ is odd. This is a filter bank structure based property and it means that every other crosstalk term is equal to zero. In addition, it has been noticed that similar terms exist in every row. These properties simplify the calculation of interference components.

5. OPTIMIZATION RESULTS

In practical FBMC systems, it is tempting to construct synthesis and analysis filter banks using a prototype filter that is as short as possible but still able to provide acceptable performance. In this manner, computational complexity, overall system delay, and transmission burst length can be minimized. There are no freely adjustable parameters for $K=1$ and $K=2$, so the most interesting overlapping factors are $K=3$ and $K=4$. An advantage of frequency sampling technique is that the same closed-form representation of (8) is valid for all values of M resulting in the scalability property. However, it has been noticed that optimum solutions can be slightly different depending on the number of subchannels. Here, the number of subchannels is selected to be $M=64$ and conclusions are drawn based on the presented results.

For $K=3$ and $K=4$, the general performance trends can be evaluated with the help of global search, i.e., we have swept realistic values of $A[1]$ using a dense grid. The generated prototype filters are analyzed based on the following performance metrics: stopband energy (SBE), minimum stopband attenuation (MSA), and total interference (TOI). Figure 2 shows the resulting levels of TOI, MSA, and SBE as a function of the adjustable parameter value $A[1]$. It can be seen that optimum value with respect to a particular metric is very easy to find, but different performance metrics are conflicting with each other. A single prototype filter cannot provide the best performance in terms of every metric. However, different kind of trade-offs can be made by selecting different value for $A[1]$.

The exact optimum solutions for design criteria C1-C4 are obtained using optimization. It should be pointed out

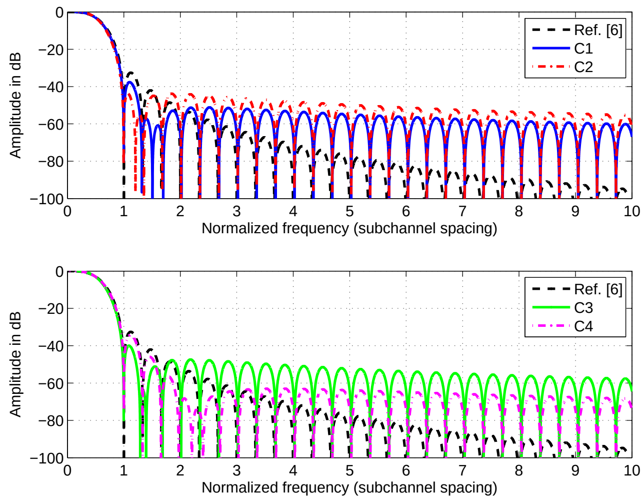

Figure 3: Magnitude responses of prototype filters in the case of $K=3$, $M=64$, and $L_p=191$.

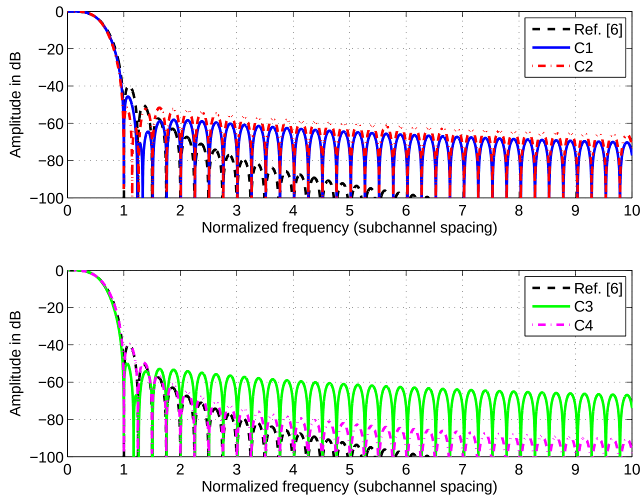

Figure 4: Magnitude responses of prototype filters in the case of $K=4$, $M=64$, and $L_p=255$.

that the optimization process is typically very sensitive to initial values. Here, we have done a set of optimizations using a random value as initial value and then the best solution has been selected. The corresponding optimum values and the resulting levels of TOI, MSA, and SBE are given in Table 1. In addition, optimized prototype filters are compared with the results presented in [6], where the authors have designed prototype filters for an 8-subchannel MDFT TMUX using the filter length of $L_p = KM+1$ (with $p[0]=0$ and $p[L_p-1]=0$). The closed-form representation of the prototype filter is similar to Eq. (8) although the authors do not identify its origin.

Figures 3 and 4 show the magnitude responses of the optimized prototype filters. The following observations can be done when comparing different designs.

- By using LS criterion, the magnitude response of the optimized filter is shaped in such a manner that the attenuation increases steadily when going further from the stopband edge. The attenuation is rather low at the stopband edge resulting in relatively high MSA level. On the other hand, LS criterion provides the second lowest TOI levels.

Table 1: Optimum values for LS (C1), minimax (C2), PCLS (C3), and total interference (C4) criteria and the resulting total interference (TOI), minimum stopband attenuation (MSA), and stopband energy (SBE) of the optimized prototype filters.

	$K=3$				$K=4$			
Criterion	$A[1]$	TOI (dB)	MSA (dB)	SBE	$A[1]$	TOI (dB)	MSA (dB)	SBE
C1	0.92492844	−41.49	−37.63	$4.19 \cdot 10^{-6}$	0.97741677	−55.13	−45.66	$5.05 \cdot 10^{-7}$
C2	0.93433197	−35.84	−43.80	$7.42 \cdot 10^{-6}$	0.98040127	−51.52	−51.69	$8.20 \cdot 10^{-7}$
C3	0.92915625	−38.71	−40.00	$4.82 \cdot 10^{-6}$	0.97972526	−52.24	−50.00	$6.90 \cdot 10^{-7}$
C4	0.91697069	−45.54	−34.30	$6.29 \cdot 10^{-6}$	0.97143701	−65.48	−39.47	$1.50 \cdot 10^{-6}$
Ref. [6]	0.91143783	−43.43	−32.57	$1.01 \cdot 10^{-5}$	0.97195983	−65.20	−39.86	$1.35 \cdot 10^{-6}$

- Minimax criterion provides evidently the lowest MSA level but this results in significantly increased total stopband energy. It is surprising that the result is not equiripple. The local minimum attenuation is almost constant only at the beginning of the stopband region but then the attenuation is steadily increasing. A drawback is the slowest overall stopband fall-off rate and high level of TOI.
- PCLS criterion provides a trade-off between LS and minimax criteria (here, $\delta = 0.01$ and $\delta = 0.00316$ for $K = 3$ and $K = 4$, respectively). The attenuation characteristics at the beginning of the stopband region are improved compared to LS design at the cost of a slightly increased TOI level.
- Total interference criterion provides evidently the lowest TOI levels. A drawback is the highest MSA levels. However, the stopband fall-off rate is clearly improved when compared to other criteria.
- It is obvious that improved stopband characteristics and decreased TOI level can be obtained by using larger overlapping factor.
- In [6], the obtained prototype filters have several desired properties such as very low level of TOI, exact stopband zeros at the frequencies that are integer multiples of the subchannel spacing, and high frequency selectivity due to superior stopband fall-off rate. It can be observed that the stopband attenuation at close distances to the transition band can be significantly increased by using other design criteria, but only with the cost of increased interference and reduced stopband fall-off rate.

6. CONCLUDING REMARKS

In this paper, prototype filter designs, which have been obtained using a frequency sampling technique, have been analyzed using a FBMC/OQAM system. In order to be able to better compare the above results with other available designs, the following observations can be given: If the filter length is increased to $L_p = KM$ or $L_p = KM + 1$ the improvement of TOI and MSA levels is marginal (only fractions of decibels). For $K = 5$, the resulting TOI and MSA levels are TOI $= [-64.4, -63.7, -71.7]$ and MSA $= [-65.2, -72.2, -56.2]$ for C1, C2, and C4 criterion, respectively.

The purpose has been to point out various performance trade-offs that can be obtained when applying different optimization criteria. Here, different prototype filters have been compared from the stopband behavior point of view because the frequency selectivity is a desired property in the context of FBMC transmission. The above analysis can be extended by utilizing new optimization criteria and performance metrics. In this manner, it is possible to take into account both the constraints and the degrees of freedom of a specific application.

REFERENCES

[1] P. P. Vaidyanathan, *Multirate Systems and Filter Banks*. Englewood Cliffs, NJ, USA: Prentice-Hall, 1993.

[2] R. van Nee and R. Prasad, *OFDM for Wireless Multimedia Communications*. London, UK: Artech House, 2000.

[3] G. Cherubini, E. Eleftheriou, and S. Olcer, “Filtered multitone modulation for very high-speed digital subscriber lines,” *IEEE J. Select. Areas Commun.*, vol. 20, pp. 1016–1028, June 2002.

[4] L. Lin and B. Farhang-Boroujeny, “Cosine-modulated multitone for very-high-speed digital subscriber lines,” *EURASIP J. Applied Signal Processing*, vol. 2006, Article ID 19329, 16 pages, 2006.

[5] P. Siohan, C. Siclet, and N. Lacaille, “Analysis and design of OFDM/OQAM systems based on filterbank theory,” *IEEE Trans. Signal Processing*, vol. 50, pp. 1170–1183, May 2002.

[6] S. Mirabbasi and K. Martin, “Overlapped complex-modulated transmultiplexer filters with simplified design and superior stopbands,” *IEEE Trans. Circuits Syst. II*, vol. 50, pp. 456–469, Aug. 2003.

[7] J. Alhava and M. Renfors, “Exponentially-modulated filter bank-based transmultiplexer,” in *Proc. IEEE Int. Symp. Circuits and Systems*, vol. IV, Bangkok, Thailand, May 2003, pp. 233–236.

[8] T. W. Parks and C. S. Burrus, *Digital Filter Design*. NY, USA: Wiley-Interscience, 1987.

[9] M. G. Bellanger, “Specification and design of a prototype filter for filter bank based multicarrier transmission,” in *Proc. IEEE Int. Conf. Acoustics, Speech, and Signal Processing*, Salt Lake City, USA, May 2001, pp. 2417–2420.

[10] P. Martín-Martín, R. Bregović, A. Martín-Marcos, F. Cruz-Roldán, and T. Saramäki, “A generalized window approach for designing transmultiplexers,” *IEEE Trans. Circuits Syst. I*, vol. 55, pp. 2696–2706, Oct. 2008.

[11] J. G. Proakis and D. G. Manolakis, *Digital Signal Processing - Principles, Algorithms, and Applications*, 3rd ed. Upper Saddle River, NJ, USA: Prentice-Hall, 1996.